Stability of Dislocation Short-Range Reactions in BCC Crystals *

Hanchen Huang [1], Nasr Ghoniem [2], Tomas Diaz de la Rubia [1], Moono Rhee [3], Hussein Zbib [3], and John Hirth [3]

[1] P.O.Box 808, L-268, Lawrence Livermore National Laboratory, Livermore, CA 94550

[2] Mechanical and Aerospace Engineering Department, UCLA, Los Angeles, CA 90024

[3] School of Mechanical and Materials Engineering, WSU, Pullman, WA 99164

ABSTRACT

The stability of short-range reactions between two dislocations of parallel line vectors which glide on two parallel slip planes in BCC crystals is determined. The two dislocations are assumed to be infinitely long, and their interaction is treated as elastic. The interaction and self-energies are both computed for dynamically moving dislocations, where the dependence on dislocation velocity is taken into account. The stability of the reaction is determined as a function of the following phase space variables: relative angle, relative speed, dislocation mobility, Burgers vector, separation of slip planes, and external force. It is found that the dynamic formation of dislocation dipoles or tilt wall embryos occurs only over a small range of the investigated phase space. Inertial effects are shown to be important at close separation, because of the large force between the two dislocations comprising the dipole or tilt wall embryo. Destabilization of the dislocation dipoles or tilt wall embryos is found to be enhanced by externally applied stresses or by stress fields of neighboring dislocations.

* Part of this work was carried out by Lawrence Livermore National Laboratory under the auspices of the US Department of Energy under contract W-7405-Eng-48

1. Introduction

In the Dislocation Dynamics (DD) methodology, plastic deformation is determined as a consequence of the motion and interaction of large collections of dislocations. As such, dislocation motion inside the solid is dictated by mutual interaction via long-range forces, as well as the externally applied stress. While the long-range interactions between dislocations may proceed at relatively long time scales, dictated essentially by the applied strain rate, short-range reactions are inevitably fast due to inherently large elastic interaction forces at close separations.

It has been shown by both experiments [1,2] and computer simulations [3,4] that short-range reactions play a pivotal role in the formation of organized deformation patterns. The walls of dislocation cells and persistent slip bands contain dislocation dipoles, which are surprisingly stable. Recently, one mechanism for the formation of dislocation dipoles has been theoretically proposed [5]. Stable dislocation dipoles have also been experimentally observed during plastic deformation of BCC Ta [6] and V [7] crystals. Dipoles can further react with other dislocations to form more complex dislocation structures. The conditions for the dynamic formation of dislocation dipoles are thus extremely important for understanding localized plastic deformation.

So far, the majority of DD models [8-13] treat the dynamics of short-range reactions in a phenomenological fashion. The models vary in their details of treating long range interactions, but generally they do not go beyond phenomenological rules when it comes to short-range reactions. These rules are indirectly inferred from experimental studies. The critical distance between two dislocations of opposite Burgers vectors below which they annihilate each other is difficult to determine. However, in copper for example, this distance is taken to be ten times the magnitude of the Burgers vector, because no dislocations separated at smaller distances have been observed under the electron microscope [12].

The dynamics of short-range reactions can be rigorously studied only when various modes of energy dissipation or exchange are taken into account. Because the elastic interaction force during short-range encounters is expected to be very large, energy dissipation or exchange mechanisms for dislocations moving close to the sound speed must be accounted for.

In this paper, we solve the equations of motion of two dislocations interacting at close range. For this purpose, we include two features which are not considered in DD simulations so far. These are: (1) the elastic interaction between the two dislocations is based on the stress fields of moving dislocations. Significant spatial distortion of the static elastic field occurs when dislocations move near their terminal sound velocity; (2) the kinetic energy of moving dislocations introduces inertial forces as a result of self-energy variations. Our studies show that these effects can be very significant.

In Section 2, we develop the governing equation of motion for relative motion of two dislocations. Using the stability theory, we define the critical separatrices separating stable dislocation reactions and bypass; the critical separatrices are defined by the initial conditions of the dislocations. We discuss applicability of the results in Section 3.

2. Formulation and Numerical Calculations

We first formulate the equation of relative motion for two infinitely-long dislocations gliding on parallel slip planes; the two dislocations have parallel line vectors and mixed characters. As an application, we solve the equation with physical parameters for a body-centered-cubic (BCC) crystal, Ta.

2.1 Equation of Motion

Since this study focuses on two idea dislocations that are infinite long and parallel, we need to develop an equation of two dimensional motion. The coordinate system for the

two dimensional motion is shown in Figure 1. To investigate their relative motion, we choose the origin of the coordinate system to move with one dislocation; this dislocation is effectively rest in our coordinate system. The two dislocations are assumed to have the same magnitude of Burgers vector, but they may have different characters. The angles between the Burgers vector and line vector of the two dislocations are α and β for the moving and rest dislocations, respectively. At any moment, the net force per unit length ($\vec{F}$) acting on the moving dislocation can be written as:

$$\vec{F} = -\frac{1}{M}\vec{v} + \vec{F}_{el} + \vec{F}_{ext} - \vec{F}_{Peierls} \quad (1)$$

where $\vec{v}$ is the dislocation velocity, the four terms on the right hand side correspond to a drag force which opposes motion, an elastic interaction force, an external force, and the Peierls barrier force. The dislocation mobility, M, is a taken to be a temperature dependent constant.

In an adiabatic motion of the dislocation, the first law of thermodynamics dictates that the change in its self-energy (W_{self}) is equal to the work done within a short distance ($d\vec{r}$). Thus [14]:

$$dW_{self} = \vec{F} \bullet d\vec{r} \quad (2)$$

where dW_{self} is the change in self-energy of the dislocation. The energy change rate is therefore given as:

$$\frac{dW_{self}}{dt} = \vec{F} \bullet \vec{v} \quad (3)$$

where the self-energy consists of the strain and kinetic components, and t is time. For a dislocation moving along a straight line on a slip plane, the self energy is an explicit function of the glide velocity [15], and equation (3) can be re-written as:

$$F = \frac{1}{v}\frac{dW_{self}}{dv}\frac{dv}{dt} = \left[\frac{1}{v}\frac{dW_{screw}}{dv} + \frac{1}{v}\frac{dW_{edge}}{dv}\right]\frac{dv}{dt} \quad (4)$$

where v is the dislocation speed, W_{screw} and W_{edge} are the self energies of screw and edge components of the dislocation, respectively. These are given as [15-17]:

$$W_{screw} = \varepsilon \frac{\cos^2 \alpha}{\gamma_t} \ln\left(\frac{R_a}{r_0}\right) \tag{5}$$

$$W_{edge} = \varepsilon \sin^2 \alpha \frac{C_t^2}{2v^2} \left[16\gamma_l + 8\gamma_l^{-1} + 2\gamma_t^{-3}(1 - 6\gamma_t^2 - 7\gamma_t^4)\right] \ln\left(\frac{R_a}{r_0}\right) \tag{6}$$

where

$$\gamma_t = \sqrt{1 - \frac{v^2}{C_t^2}}, \quad \gamma_l = \sqrt{1 - \frac{v^2}{C_l^2}} \tag{7}$$

and $C_t = \sqrt{\frac{\mu}{\rho}}$ is the transverse speed of sound, $C_l = \sqrt{\frac{2\mu + \lambda}{\rho}}$ is the longitudinal speed of sound, $\varepsilon = \frac{\mu b^2}{4\pi}$ is an energy factor, b is the magnitude of the Burgers vector, μ and λ are Lame's constants, ρ is the mass density of the solid, R_a is a cutoff distance of elastic energy (usually taken as the crystal or microstructure dimension), and r_0 is the core radius of the moving dislocation.

Upon differentiation of equations (5) and (6) with respect to v, we obtain:

$$\frac{1}{v}\frac{dW_{screw}}{dv} = \varepsilon \cos^2 \alpha \frac{1}{\gamma_t^3 C_t^2} \ln\left(\frac{R_a}{r_0}\right) \tag{8}$$

and

$$\frac{1}{v}\frac{dW_{edge}}{dv} = \frac{\varepsilon \sin^2 \alpha C_t^2}{v^4} \left[7\gamma_t + 25\gamma_t^{-1} - 11\gamma_t^{-3} + 3\gamma_t^{-5} - 8\gamma_l - 20\gamma_l^{-1} + 4\gamma_l^{-3}\right] \ln\left(\frac{R_a}{r_0}\right) \tag{9}$$

The ratio of the inertial force and dislocation acceleration can be interpreted as the effective mass. It is noted here that in the low velocity limit, equations (8) and (9) reduce to those for the effective mass of screw and edge dislocations, respectively, as introduced by Frank [16] and Weertman [17]. However, we do not use the effective mass formulation here and replace it with a more general energy approach, as given by equations (1), (4), (8), and (9) above.

Starting with the stress field of a moving dislocation given in reference [15], the elastic interaction force along the glide direction (i.e., x direction in Figure 1) is shown to be:

$$F_{el} = \varepsilon \frac{2x}{r_t^2}\left\{\gamma_t \cos\alpha\cos\beta - \sin\alpha\sin\beta\frac{C_t^2}{\gamma_t v^2}\left[\left(1+\gamma_t^2\right)^2 - \gamma_t\gamma_l\frac{4r_t^2}{r_l^2}\right]\right\} \tag{10}$$

Using equations (1)-(10) and introducing the dimensionless variables $F'_{ext} = F_{ext}\frac{b}{\varepsilon}$, $M' = M\frac{\varepsilon}{bC_t}$, $V = \frac{v}{C_t}$, $X = \frac{x}{b}$, $R_t = \frac{r_t}{b}$, and $R_l = \frac{r_l}{b}$, the equation of motion (equation 4) can now be given in the following explicit form:

$$K\frac{dV}{dX}\ln\left(\frac{R_a}{r_0}\right) = -\frac{V}{M'} + F'_{ext} + \Gamma \tag{11}$$

where

$$K = \frac{\sin^2\alpha}{V^3}\left[7\gamma_t + 25\gamma_t^{-1} - 11\gamma_t^{-3} + 3\gamma_t^{-5} - 8\gamma_l - 20\gamma_l^{-1} + 4\gamma_l^{-3}\right] + \cos^2\alpha\frac{V}{\gamma_t^3} \tag{12}$$

and

$$\Gamma = \frac{2X}{R_t^2}\left\{\gamma_t\cos\alpha\cos\beta - \sin\alpha\sin\beta\frac{1}{\gamma_t V^2}\left[\left(1+\gamma_t^2\right)^2 - \gamma_t\gamma_l\frac{4R_t^2}{R_l^2}\right]\right\} \tag{13}$$

It is noted that the dimensionless equation of dislocation motion, equation (11), is highly non-linear in the velocity. Solutions of this equation will be considered for short-range reactions where the pair elastic interaction of the two dislocations dominates. Any measurable effects due to the Peierls barrier are assumed to be included in the external force. The influence of the effective external force on the stability of the short-range reaction will also be studied in the following section.

2.2 Numerical Results for BCC Crystals

As an application of this work, we study short-range reactions in a BCC crystal, Ta. For a BCC crystal, the angles α and β are related, since a Burgers vector can only be

one of the $\frac{1}{3}<111>$ vectors. On any given {110} slip plane, there are four possible combinations of the Burgers vectors for the two dislocations. Because the line vectors of the two dislocations are identical, β can take only one of the following four possible values:

$$\beta = \begin{cases} \alpha \\ \alpha + 180^0 \\ \alpha + 120^0 \\ \alpha + 300^o \end{cases} \qquad (14)$$

The dislocation mobility has been measured to be 4.2×10^4 (Pa sec)$^{-1}$ in Nb at room temperature [18]; the dislocation character was not identified in this work. A much smaller value, 3.3×10^3 (Pa sec)$^{-1}$, was obtained by Urabe and Weertman [19] for edge dislocation mobility in Fe. According to Urabe and Weertman [19], the mobility of screw dislocations in Fe is only about a factor of two smaller than that of edge dislocations near room temperature. Based on these experimental observations, we estimate the dislocation mobility to be in the range of 10^3 to 10^5 (Pa sec)$^{-1}$ in BCC crystals. In this work, we choose 10^5 (Pa sec)$^{-1}$ as the reference value for the mobility of dislocations, regardless of their character. The sensitivity of the results to dislocation mobility is tested by performing calculations using a lower mobility (10 times lower). Taking $\mu = 69$ GPa, $\rho = 16600$ kg/m^3, and b=2.86 Å for Ta [20,21], we estimate that M' is about 50. Unless otherwise mentioned, we use $\lambda = 149$ GPa [21], $R_a = 10000b$, $h = 10b$, F=0, and $r_0 = 4b$ in this study. The cutoff radius, R_{cut}, shown in Figure 1 is chosen to be 500b so that pair interaction of the two dislocations dominates over interactions with other neighbors. As the angle β is shifted by 120^o, the shape of elastic interaction field is not affected if the coordinate α is also shifted. Therefore, the following analysis will focus on two of the four possible combinations: (1) two dislocations are parallel (parallel line vectors and same Burgers vector); and (2) the two dislocations are anti-parallel (parallel line vectors and opposite Burgers vectors).

2.2.1 Stable Dislocation Structures

To find stable dislocation structures, we first calculate constant force contours for two parallel dislocations at zero velocity; the results are shown in Figure (2a). When α is close to 90^o, the zero force configuration at $\theta=90^o$ is stable since a small deviation from this configuration will be restored by the elastic interaction force. For example, if the moving dislocation is given a small positive displacement away from $\theta=90^o$ along the x direction, it will be accelerated towards $\theta=90^o$ by the elastic interaction force. In contrast, the other zero force configurations are unstable because the elastic interaction force amplifies a deviation of any small magnitude. As a result, two parallel dislocations can form a stable cluster with one dislocation on top of the other with $\theta=90^o$. To form such a stable cluster, the two dislocations must be close to be edge in character. A special case is the formation of a tilt wall embryo when the two dislocations are pure edge in character.

The elastic stress field for two anti-parallel dislocations are opposite in sign to that for two parallel ones. As shown in Figure (2b), the constant force contours are similar to those of Figure (2a). Zero force configurations are the same, but the non-zero force values have the opposite sign. As a result, the zero force configurations which are stable for two parallel dislocations are unstable for two anti-parallel ones, while those which are unstable for two parallel dislocations are stable here. When the two dislocations are close to be edge in character, they can form a stable cluster with one on either side of the other. As a special case, two anti-parallel edge dislocations can form a dipole at either $\theta=45^o$ or $\theta=135^o$. If the two dislocations are close to be screw in character, they can form a stable cluster only with one on top of the other. This configuration is similar to that of the tilt wall embryo. However, the two dislocations which are close to the screw character may rotate themselves to facilitate cross-slip. Because of the high probability of cross-slip for screw dislocations in BCC crystals, this stable configuration will not be given further consideration.

As a dislocation moves at a high speed, its elastic stress field deforms with respect to a stationary observer. The elastic interaction force field of the two dislocations also deforms. This effect is shown in Figure (3a) for two parallel dislocations. Comparing Figure (2a) and (3a), we note that these elastic interaction fields behave in a similar fashion, although the locations of the zero force configurations are shifted. A similar behavior is observed when we compare Figures (3b) and (2b) for two anti-parallel dislocations. Therefore, stability analyses for zero velocity and finite velocity dislocation interactions are similar.

2.2.2 Typical Trajectories for the Moving Dislocation

For the special case of two anti-parallel edge dislocations, we study the trajectories of their relative motion with various initial conditions. The position and velocity of the moving dislocation are traced for three different initial velocities (all are scaled to the transverse speed of sound): (1) V_0=0.8; (2) V_0=0.6; and (3) V_0=0.5. The initial position for all the three cases are the same, i.e., they all start at $\theta=60^o$. As shown in Figure (4a), the moving dislocation with an initial velocity of 0.8 heads towards the right and cross the cut-off circle defined by $r R_{cut}$. The pair interaction is relatively weak beyond the cut-off distance, and the moving dislocation is considered as having bypassed the rest one in this study. For a smaller initial velocity (0.6), the moving dislocation converges to $\theta=45^o$ which corresponds to one dipole configuration, after crossing the symmetrical position $\theta=90^o$ four times. For an even smaller initial velocity (V_0=0.5), the moving dislocation converges to $\theta=135^o$ which corresponds to the other dipole configuration, after crossing the symmetrical position $\theta=90^o$ three times. It is interesting to note that the initial positions of the three trajectories are identical. The final positions of the moving dislocation are entirely different because the initial velocities are different. This indicates that the phenomenological rules which are based on separation or force in the DD methods [8-13] must be modified to account for the effects of detailed dynamics on the final stability.

As shown in Figure (4b), tracing the dipole formation at $\theta=45^o$ takes more than 35000 integration steps before the trajectory converges to $\theta=45^o$ within 1^o, if the maximum displacement in each integration step is limited to 0.1b. Although implicit numerical integration methods may reduce the number of integration steps by an order of magnitude, the computational effort is still enormous. During a DD simulation, only a few integration steps can be afforded for a dislocation to move 500b.

To account for the velocity dependence during short-range reactions and keep the DD simulations computationally feasible, a bridging method is necessary. As can be seen in Figures (4a) and (4b), there must be a critical initial velocity between 0.6 and 0.5, slightly below which a dipole forms at $\theta=135^o$ and slightly above that a dipole forms at $\theta=45^o$. The trajectory corresponding to the critical velocity is a separatrix. It is therefore desirable to determine all such separatrices in order to predict the final configuration of two reacting dislocations according to their initial conditions. In the following sub-sections, we define the critical separatrices and present numerical results for short-range reactions involving two parallel or anti-parallel dislocations.

2.2.3 Formation of Tilt Wall Embryos

For simplicity of presentation, we use two pure edge dislocations for description of the critical separatrices. As indicated by the elastic interaction force, the solid line in Figure 5, a tilt wall embryo can be formed at $\theta=90^o$. To form such a tilt wall embryo, the moving dislocation must be able to approach the stable configuration and be trapped there. Therefore, the following conditions must be satisfied:

(1) The moving dislocation must not cross the zero force configuration at $\theta=45^o$ if it moves towards the right, i.e., V 0 at $\theta=45^o$. Otherwise, the dislocation will cross $\theta=45^o$ and it will be further pushed away from the rest dislocation by the repulsive force at $\theta>45^o$.

(2) The moving dislocation must be able to cross the zero force configuration at $\theta=45^o$ if it moves towards the left, i.e., V 0 at $\theta=45^o$. Otherwise, it will not approach the stable configuration due to the repulsive force at $\theta>45^o$.

(3) Similar to condition (1), the moving dislocation must be V 0 at $\theta=135^o$ if it heads towards the $\theta=135^o$ from right.

(4) Similar to condition (2), the moving dislocation must be V 0 at $\theta=135^o$ if it heads towards the $\theta=135^o$ from left.

By setting the final velocity to zero according to the four conditions above and solving equation (11) backwards in time, we obtain the critical separatrices for two parallel edge dislocations, as shown in Figure (6a). The area enclosed by the four critical separatrices is a stable domain, and the rest are unstable. If the moving dislocation starts with an initial condition that is within the stable domain, a tilt wall embryo will result regardless of how the two dislocations approach each other.

2.2.4 Formation of Dislocation Dipoles

Similar to the analysis of tilt wall embryo formation, we describe dipole formation using two anti-parallel pure edge dislocations. The elastic interaction force of two dislocations as a function of their relative position is shown in Figure (5) as a dotted line. There are two stable configurations for the dipole, in contrast to one stable configuration for the tilt wall embryos. Due to the symmetry, we will only discuss the critical separatrices for dipole configurations at $\theta=45^o$. The critical separatrices for the other dipole configuration can be obtained by a transformation of θ to $(180^o-\theta)$ and V to (-V). In order to form a dipole at $\theta=45^o$, the moving dislocation must be able to approach this stable configuration and be trapped there. Therefore, the following conditions must be satisfied:

(1) The moving dislocation must come to rest before reaching the cut-off circle (indicated by θ_R in Figure 5), if it moves towards the right, i.e., V 0 at $\theta=\theta_R$. Otherwise,

the moving dislocation is taken as having bypassed the rest one and will be treated by the DD simulations.

(2) The moving dislocation must come to rest as it approaches $\theta=90^o$ from the right at the final stage, i.e., V 0 at $\theta=90^o$. It is worth mentioning here that this condition need not to be satisfied every time the moving dislocation approaches $\theta=90^o$. In fact, the moving dislocation can cross $\theta=90^o$ several times, as shown in Figure (4a) before finally converging to the stable position at $\theta=45^o$.

Setting the final condition to be V=0 according to the two conditions above and solving equation (11) backwards in time, we obtain the critical separatrices for dipole formation at $\theta=45^o$. By using the symmetrical transformation, we also derive the critical separatrices for dipole formation at $\theta=135^o$. The results are shown in Figure (6b). The two solid lines at θ_R and θ_L merely indicate the border of the phase space we are interested in (i.e., the phase space within the cutoff circle).

If the moving dislocation starts with an initial condition corresponding to the shaded area in Figure (6b), it is determined to form a dipole with the rest dislocation at $\theta=45^o$. It is interesting to note that a small perturbation of either velocity, position, or both can change the dipole configuration from $\theta=45^o$ to $\theta=135^o$ or vice versa.

2.2.5 Sensitivity Analyses

So far, this section has been devoted to the analysis of two edge dislocations with a constant dislocation mobility, a zero external force and a constant separation of slip planes. The effects of these four factors are investigated by varying them in equation (11).

As the two dislocations become mixed in character, the fraction of stable domains may change. Taking the angle α to be 45^o, we calculate the critical separatrices and plot them in Figures (7a) and (7b) for two parallel and anti-parallel dislocations, respectively. The only difference between Figures (6) and (7) is the angle α. For two parallel

dislocations, it is easy to see that a much smaller fraction of the phase space is stable when the angle α is away from 90^o. In other words, two parallel edge dislocations are much more likely to form a tilt wall embryo than two parallel dislocations of mixed character. The fraction of stable domains for two anti-parallel dislocations is not strongly dependent on the angle α. However, the partition of the stable domain is much finer when α is away from 90^o. As a result, an even smaller perturbation in either velocity, position, or both will change the final stable configuration from $\theta=45^o$ to $\theta=135^o$ or vice versa. This work shows that stable dipoles and tilt wall embryos still form if dislocations are of a mixed character, although under much more restrictive conditions. This finding expands the well-known concept of dipole and tilt wall formation for only edge character dislocations.

To investigate effects of dislocation mobility on the stability analyses, we repeat the calculations for Figure (6) with a mobility that is ten times smaller. The critical separatrices for two parallel and anti-parallel edge dislocations are shown in Figures (8a) and (8b), respectively. Comparing Figures (6) and (8), we note that: (1) the fraction of the stable domain is much larger with a lower mobility, for both parallel and anti-parallel dislocations; and (2) the partition of the stable domain for two anti-parallel dislocations is much coarser. These effects are attributed to the more efficient energy dissipation with a lower mobility.

A non-zero external force can enhance or reduce the formation of a stable dislocation cluster. Qualitatively, increasing the separation H is similar to decreasing the mobility, since both give rise to a smaller net force on the moving dislocation. Therefore, we demonstrate the effects of the external force and the separation H on the stability analysis by studying a critical condition when no stable configuration exists. As shown in Figure (5), the maximum magnitude of the elastic force at H=10 is 0.076. If an external force of this magnitude or larger is applied, the total force will be either positive or negative everywhere. With the elimination of all zero force configurations, a stable cluster will never form. Taking the critical external force as the maximum magnitude, we calculate it as a function of the separation H. As shown in Figure (9), a strong external force

(greater than 0.01) is needed to eliminate all zero force configurations as the separation is smaller than 50b. However, a much smaller external force have the same effects at a larger separation.

3. Conclusions and Discussions

Inertial effects on dislocation interactions are accounted for by balancing the elastic self energy change of the moving dislocation with the work done on it. It is worth mentioning that this treatment is general and applies to both high and low velocities. In the low velocity limit, the treatment is identical to that given in references [16,17]. The inertial effects are extremely important during short-range reactions, although they may play a minor role during slow motion of dislocations. The trajectory with an initial velocity of 0.6 in Figure (4a) is reproduced without considering the inertial effects (setting the inertial force to be zero). The result is shown in Figure 10, together with the trajectory in Figure (4a) for comparison. It is noted that the moving dislocation reaches an unreasonably high speed (about four times the transverse speed of sound) during a short-range reaction if inertial effects are omitted. Therefore, large errors in DD can be expected if the inertial effects are ignored.

The results presented in Section 2 are based on solutions of a dynamic equation which takes inertial effects into account. It might appear that one can directly solve this equation in DD simulations. However, the moving dislocation does not approach a minimum energy configuration directly even if it starts from a stable domain. Instead, it oscillates many times before converging onto a stable position. Therefore, it takes an intensive computational effort to track the trajectory of the moving dislocation. As shown in Figure (4b), it takes 35000 integration steps before the trajectory converges to $\theta=45^{o}$ within 1^{0}. In a DD simulation, only several integration steps are taken for a dislocation to displace 500b in order to simulate plastic deformation of relevant strains and strain rates. Therefore, it is necessary to develop physical rules of short-range reactions and use them

as input in DD simulations. This can be accomplished by using the results of stability analyses, as presented in this work.

The critical separatrices can be parameterized in terms of dislocation character, position, velocity, mobility, and external force. A look-up table can therefore be generated and used as input for DD simulations. In DD simulations, two dislocations which are within R_{cut} are checked for short-range reactions according to their characters, positions, velocities, mobility, and external forces. If the state defined by these parameters fall into a stable domain, they will immediately be brought to the corresponding stable configuration, such as a tilt wall embryo or a dipole configuration. Otherwise, their trajectories are updated according to the DD methods. Such a bridging method enables DD simulations to capture details of dislocation microstructure evolution without a substantial sacrifice of computational efficiency.

As demonstrated in Section 2, the external force can eliminate configurations of stable dislocation clusters. In DD simulations, the external force is defined as the total force from external loading and from interaction with all other dislocations excluding the one in short range reaction. When the two dislocations are very close, the change of their elastic interaction energy as a function of the angle θ comes mainly from the pair interaction. The elastic interactions with other dislocations, if they are relatively far away, do not change much as a function of the angle θ. Therefore, it is reasonable to treat contributions from other neighboring dislocations as a constant external force in studying stability of dislocation short-range reactions.

This study aims at illustrating the necessity of investigating short range interactions in details. Therefore, several assumptions have been made without rigorous justifications, and these will be discussed here. First, the character of the two dislocations are assumed to be fixed during the short-range reaction. A dislocation can rotate during its motion depending on the net force on it; therefore, the two dislocations will not always stay parallel. The second severe assumption is that the two dislocations always glide on parallel

slip planes. Cross-slip of pure screw dislocations is therefore excluded in the model. Even if the dislocations are edge or mixed type in character, they can climb under their high mutual stress, which is possible during the short-range reactions. Third, the mobility of dislocations should depend on the dislocation character, which is not considered in this work. Finally, the velocity dependence of elastic stress field is assumed to propagate at infinite speed. We will generalize the present work to alleviate these restrictions in future studies.

Acknowledgment

One of the authors (Huang) thanks D. Lassila, L. Hsiung, and G. Campbell for providing many important experimental results, and J. Shu for stimulating discussions on bridging micro and meso length scales.

References:

1. H. Muhgrabi, 1971, **Phil. Mag. 23,** 897
2. H. Chen, J. Gilman, and A. Head, 1964, **J. Appl. Phys. 35**, 2502
3. N. Ghoniem and R. Amodeo, 1990, in **Patterns, Defects and Materials Instabilities**, edited by D. Walgraef and N. Ghoniem, (Kluwer Academic Publishers, the Netherlands) p 303.
4. L. Kubin, 1993, **Phys. Stat. Sol. (a) 135**, 433
5. J. Gilman, 1997, **Phil. Mag. A 76**, 329
6. L. Shiung, 1997, private communication
7. R. Arsenault, 1975, in **Plastic Deformation of Materials**, edited by R. Arsenault (Academic Press, New York) p 1
8. R. Amodeo and N. Ghoniem, 1990, **Phys. Rev. B. 41**, 6958
9. R. Amodeo and N. Ghoniem, 1990, **Phys. Rev. B. 41**, 6968
10. H. Zbib, M. Rhee, and J. Hirth, 1997, **Int. J. Mech. Sci 39**, in press
11. M. Rhee, H. Zbib, J. Hirth, H. Huang, T. Diaz de la Rubia, 1997, submitted to **Modelling Simul. Mater. Sci. Eng.**
12. L. Kubin, 1993, in **Treatise in Materials Science and Technology**, edited by R. Cahn, P. Hassan, and E. Kramer, Weinhum, (VCH: Weinhum FRG) p 138
13. G. Canova, Y. Brechet, L. Kubin, B. Devincre, V. Pontikis, and M. Condat, 1994, **Solid State Phenomena 35-36**, 101
14. J. Hirth and J. Lothe, 1982, **Theory of Dislocations**, second edition (John Wiley & Sons, New York) Chapter 5
15. J. Lothe, 1992, in **Elastic Strain Fields and Dislocation Mobility**, edited by V. Indenbom and J. Lothe, (North-Holland, New York) p 447
16. F. Frank, 1949, **Proc. Phys. Soc. A62**, 131
17. J. Weertman, 1961, in **Response of Metals to High Velocity Deformation**, edited by P. Shewmon and V. Zackay, (Interscience Publisher, New York) p 205
18. W. Mason and D. MacDonald, 1936, **J. Appl. Phys. 42**, 1836
19. N. Urabe and J. Weertman, 1975, **Mater. Sci. Engr. 18**, 41

20. S. Cardonne, P. Kumar, C. Michaluk, and D. Don Schwartz, 1992, **Advanced Materials & Processes 9,** 16

21. H. Boyer and T. Gall, 1985, **Metals Handbook® Desk Edition**, (American Society for Metals, Metal Park, Ohio) p2.16

Figure Caption:

Figure 1: Coordinate system and configuration of the two reacting dislocations. The center of the coordinate system coincides with the reference dislocation.

Figure 2: Contours of constant force for (a) parallel; and (b) anti-parallel dislocations.

The five contours are for the reduced elastic force (F_{el}/ε) equal to -10^{-2} (“ ”), -10^{-3} (“ ”), 0 (“ ”), 10^{-3} (“ ”), and 10^{-2} (“ ”), respectively.

Figure 3: (a) Zero interaction force configurations for two parallel dislocations with V

equal to 0.0 (“ ”), 0.5 (“ ”), and 0.9 (“ ”), respectively; (b) Deformed contours of constant interaction force for the two

parallel dislocations with V equal to 0.9, with the legends the same as in Figure (2a).

Figure 4: Typical phase space trajectories with initial θ at 60^{o} and V=0.5 (“ ”),

0.6 (“ ”), and 0.8 (“ ”), respectively. The velocity as a function of the angle θ is shown in (a), and the number of integration steps as a function of θ is shown in (b).

Figure 5: Static elastic interaction force as a function of the angle θ for two parallel edge dislocations (“ ”), and anti-parallel edge dislocations (“ ”), respectively.

Figure 6: Critical separatrices for (a) two parallel edge dislocations, and (b) two anti-

parallel edge dislocations.

Figure 7: Critical separatrices for (a) two parallel dislocations with $\alpha=45^{o}$, and (b) two anti-parallel dislocations with $\alpha=45^{o}$.

Figure 8: Critical separatrices for (a) two parallel edge dislocations with $M'=5$, and (b) two anti-parallel edge dislocations with $M'=5$.

Figure 9: Critical external force necessary to eliminate all stable configurations as a function of separation of slip planes.

Figure 10: Comparison of two trajectories: (1) that with an initial velocity of 0.6 as in Figure (4a) ("——"); and (2) that with the same condition but omitting the inertial effects ("——").

Figure 1: Huang et al

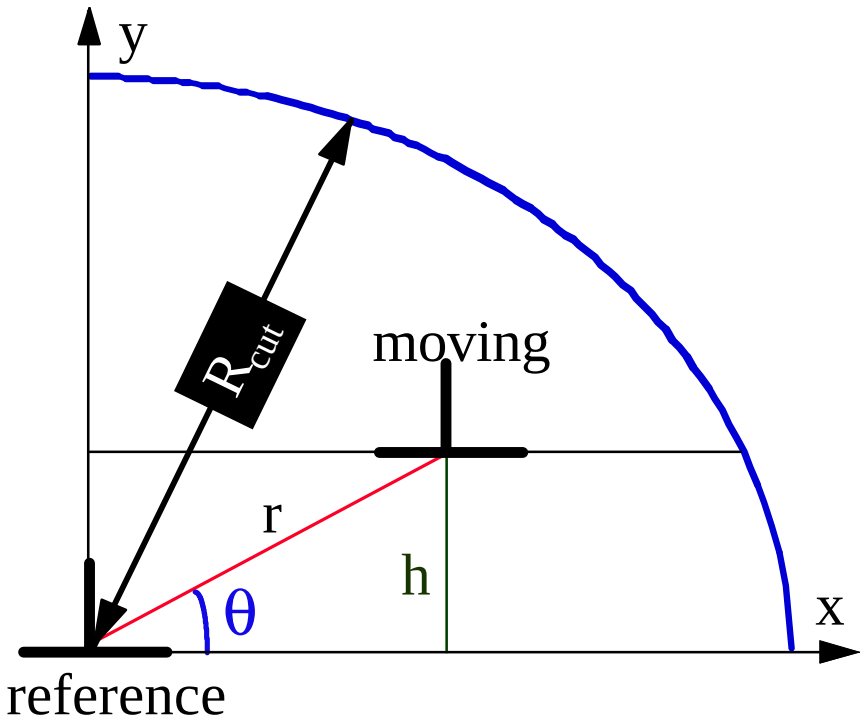

Figure 2a: Huang et al

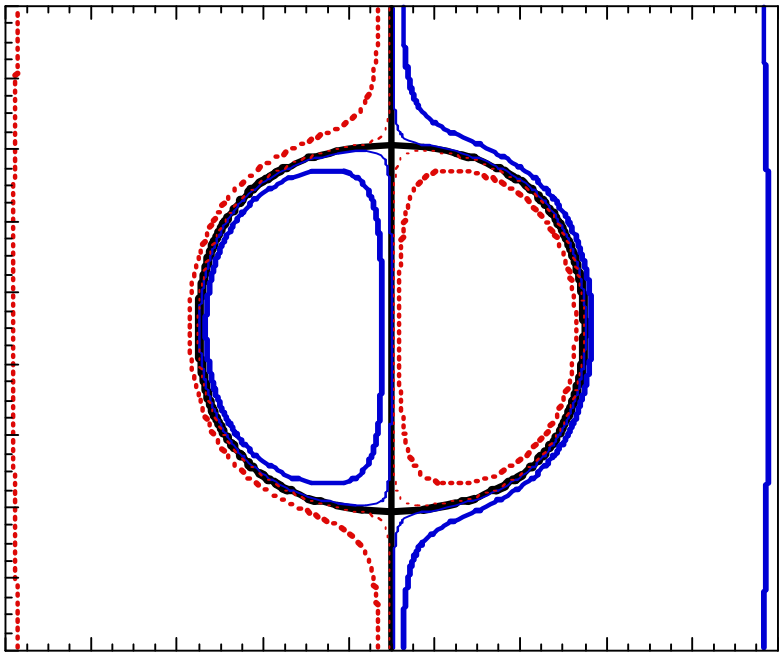

Figure 2b: Huang et al

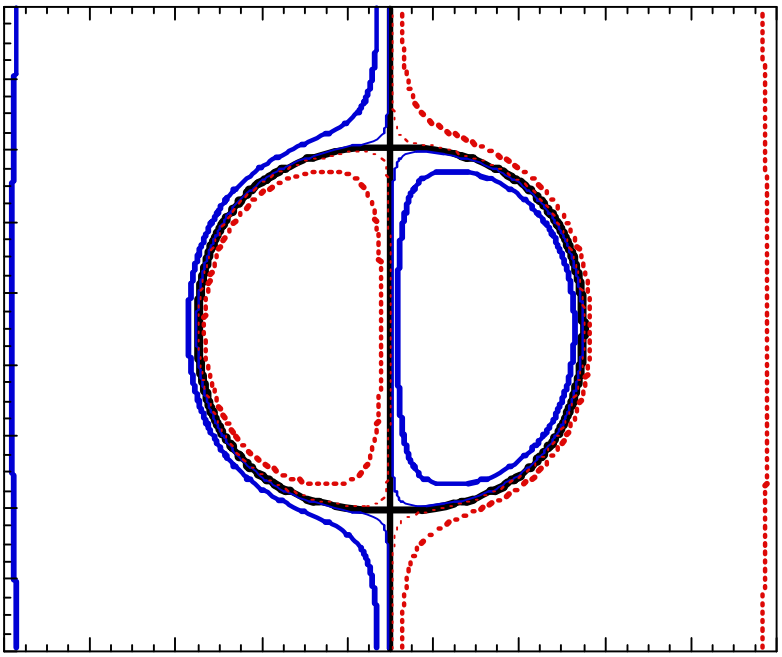

Figure 3a: Huang et al

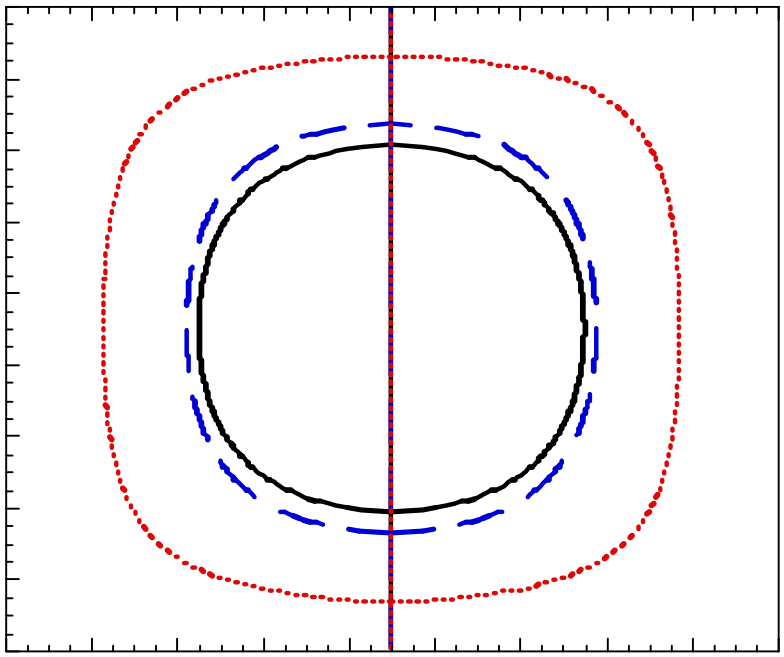

Figure 3b: Huang et al

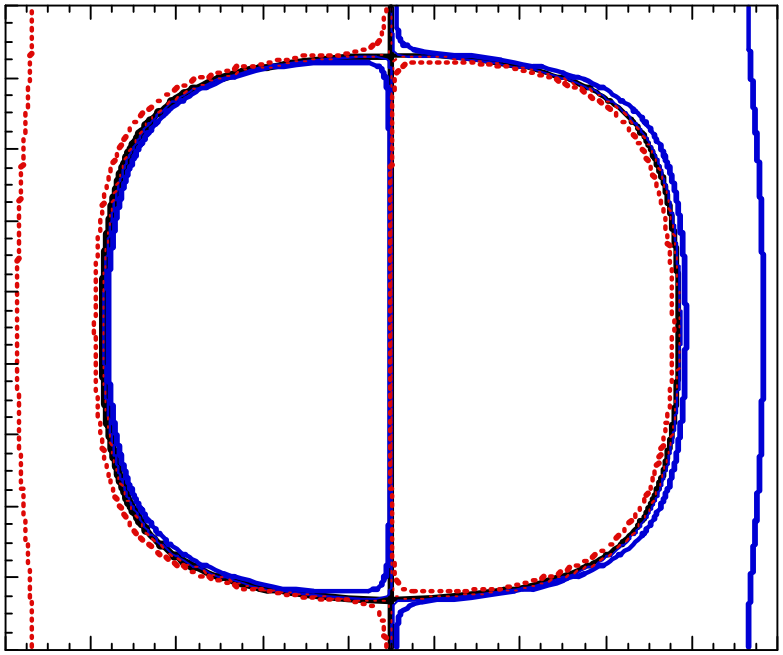

Figure 4a: Huang et al

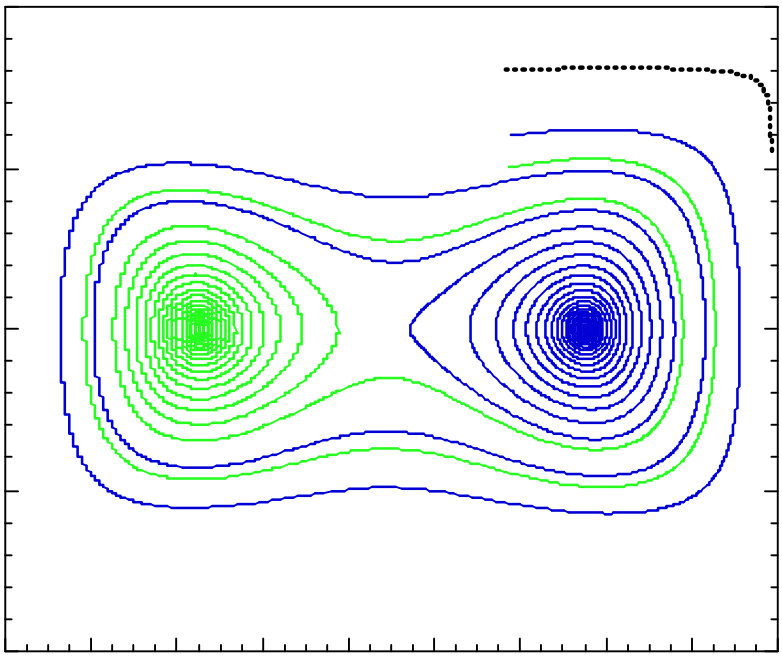

Figure 4b: Huang et al

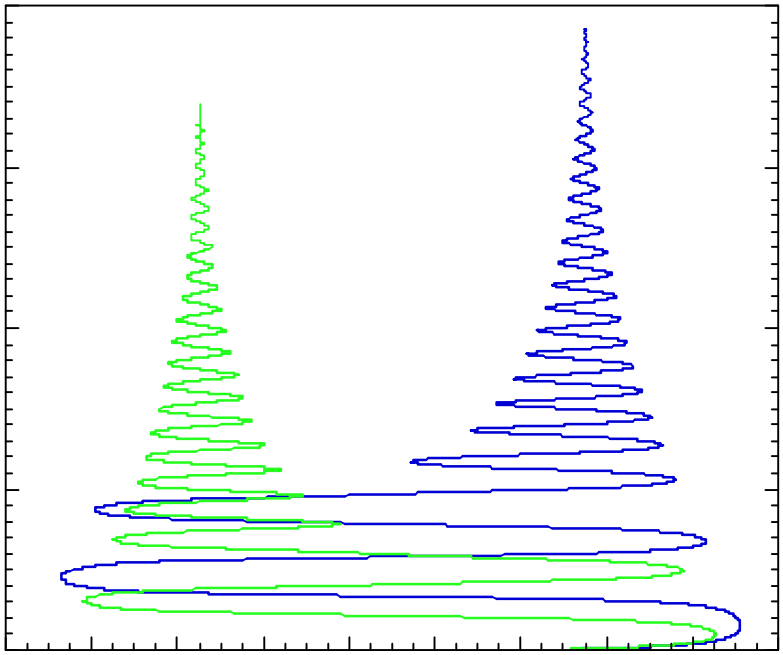

Figure 5: Huang et al

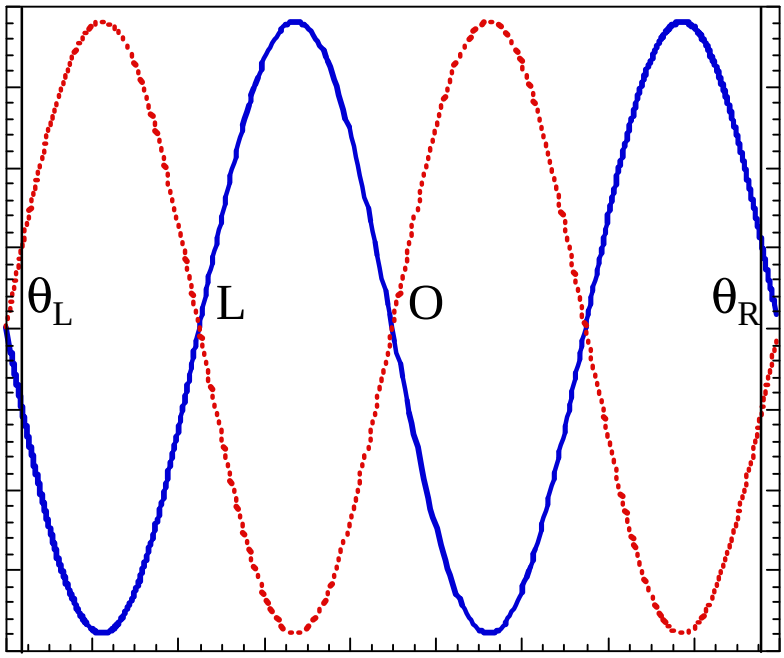

Figure 6a: Huang et al

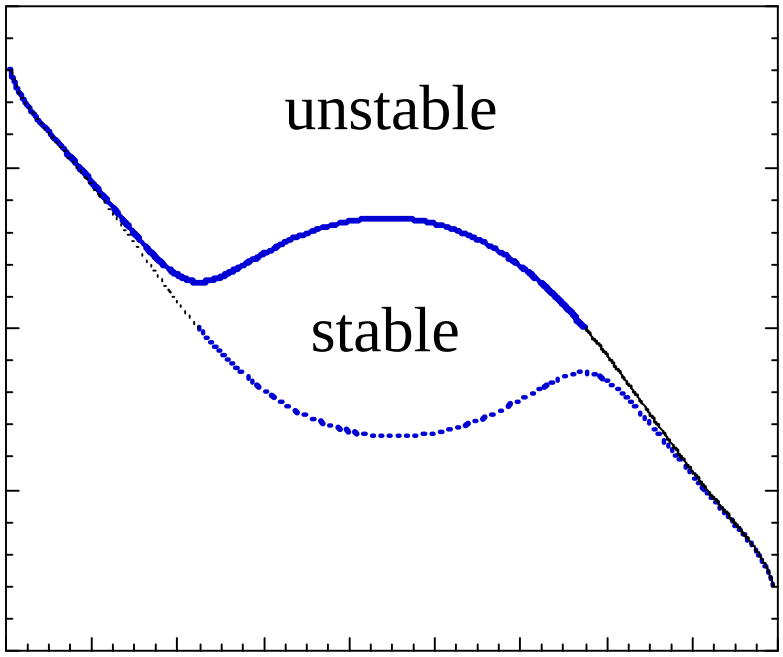

Figure 6b: Huang et al

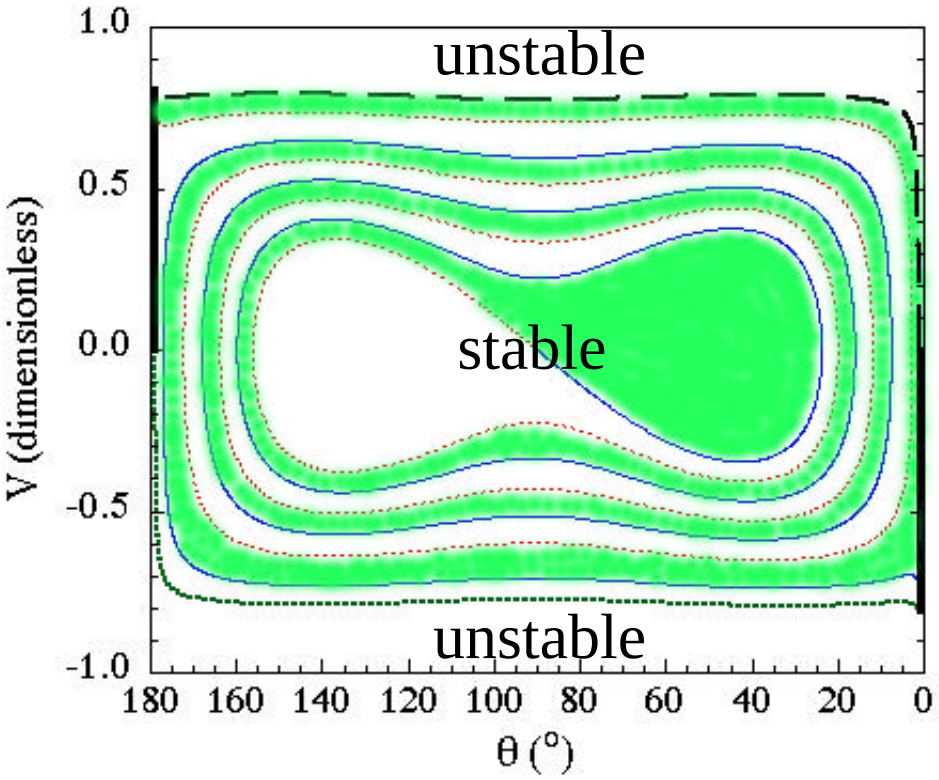

Figure 7a: Huang et al

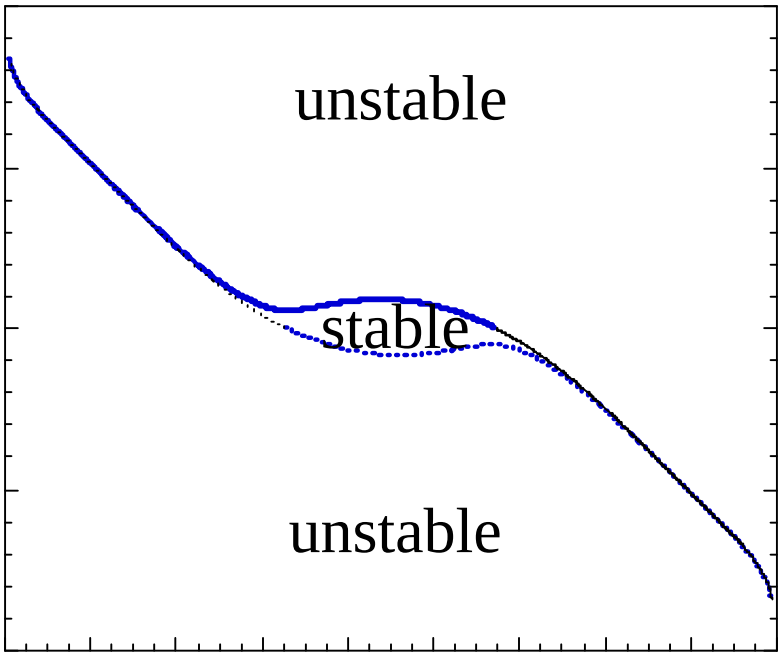

Figure 7b: Huang et al

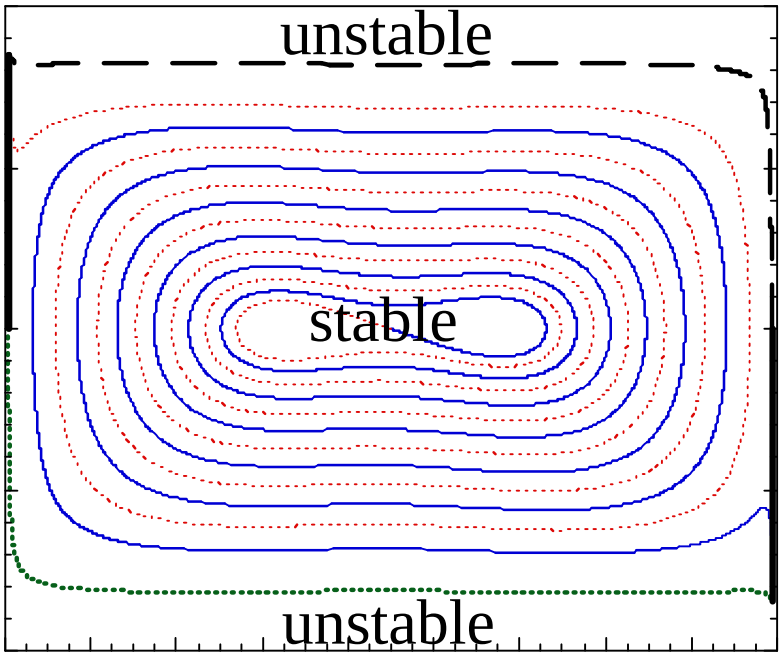

Figure 8a: Huang et al

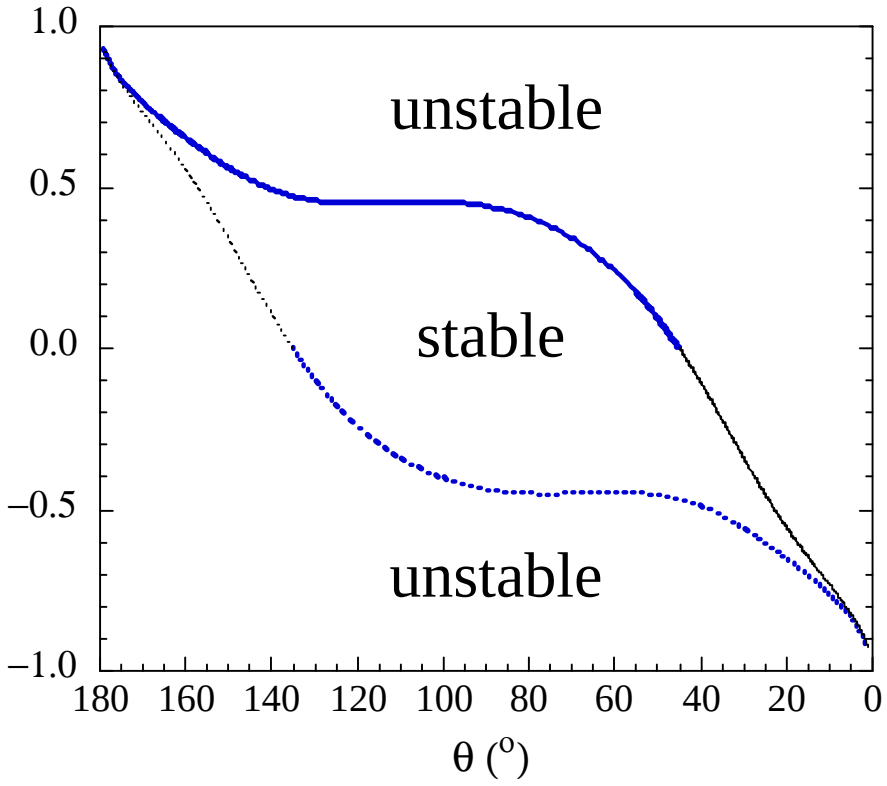

Figure 8b: Huang et al

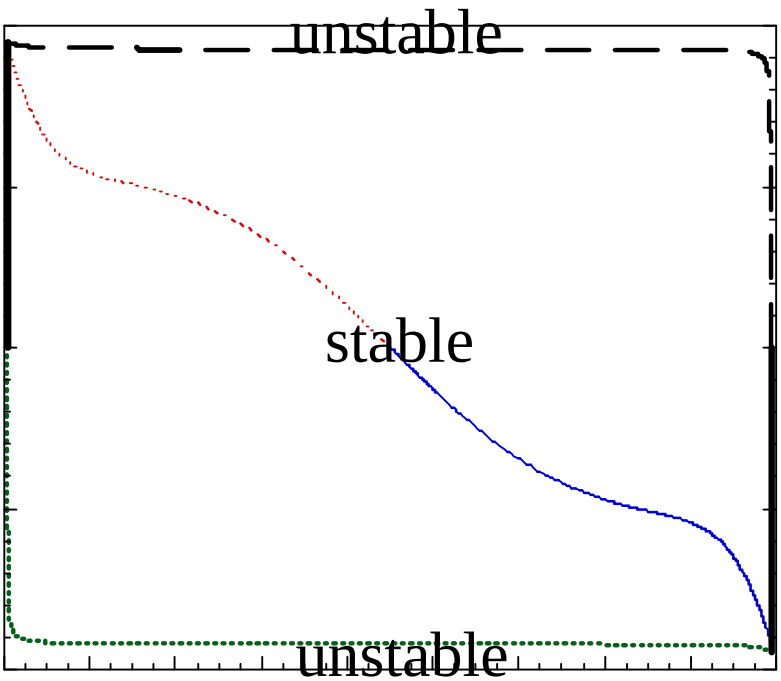

Figure 9: Huang et al

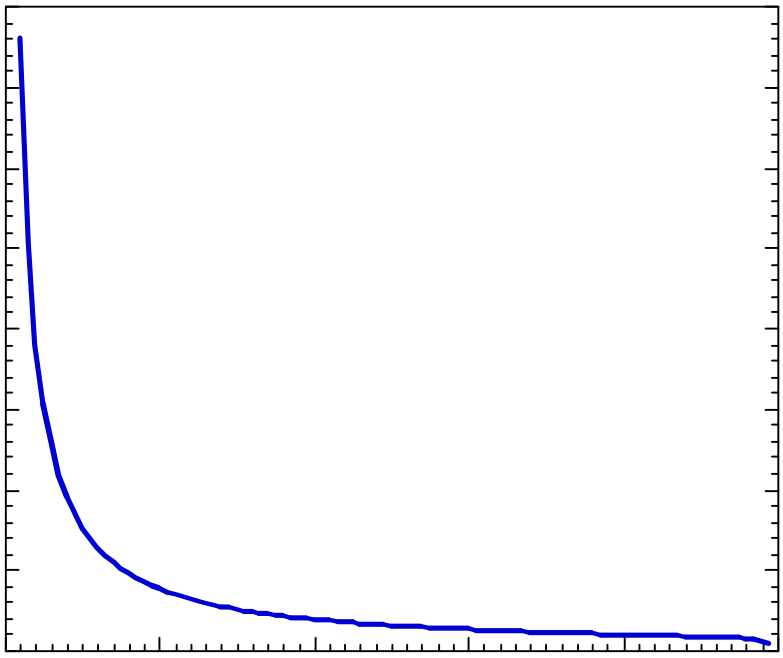

Figure 10: Huang et al